SAND2020-10706C

Vapor Transport Analysis of a Chloride Molten Salt Flow Control Valve

Kenneth M. Armijo[1], Hector Mendoza[1] and Jeffrey Parish[2]

[1]Concentrating Solar Technologies Department 8823, Sandia National Laboratories, PO 5800 MS 1127, Albuquerque NM, USA 87185
[2]Flowserve Corporation, 1350 North Mountain Springs Parkway, Springville, UT 84663, USA.

1. Abstract

This investigation explores thermal-fluid flow phenomena in a proportional flow control valve (FCV) within a 2 in. ID high-temperature piping transport system. The FCVs are critical components to ensure flexible nominal operation of a 2 MW_{th} concentrating solar power (CSP) pilot-scale system in present development at Sandia National Laboratories (SNL). A computational fluid dynamics (CFD) / finite element analysis (FEA) model was developed in ANSYS that investigates multifluid phase-change transport within various sections of an FCV to explore plating and subsequent thermal-mechanical stress challenges that can exist with operations as high as 730 °C. Preliminary results from the thermal-fluid model in development suggest salt vapor phase change in the N_2 gas purge lines as low as approximately 476 °C, which can have a negative impact on valve reliability.

2. Introduction

Proportional control valves are required to modulate flow through a CSP system in order to facilitate operational modes required for preheating a receiver, thermal energy storage (TES) charging, and system drain-back operations. Proper flow control through an FCV is also critical for fine resolution pump flow management when operating variable flow devices (VFD) at their lower limits operations for preheating power block heat exchangers (HX). However, salt wicking and reliable seal challenges may persist with FCVs operating at high-temperatures where thermal-mechanical expansion and relaxation challenges can exist for both packing and bellows seal options. Previous multi-phase valve designs researched by Smith et al. [1] noted that although bellows seals can reduce salt wicking for smaller valves, the complexity and costs make these types of seals difficult to scale to commercially. Therefore, the authors noted that particular packing configurations with extended bonnets and high-temperature materials can instead be employed to reduce salt wicking and leaks. However, in later SNL National Solar Thermal Test Facility (NSTTF) studies of larger 6 in. valves [2], researchers found persistent challenges with packing thermal management that later led to leakage. The employment of ullage gas purge lines has indicated salt leak reduction through the packing can be possible [3]. Although molten salt valve designs such as those by Flowserve Corp. have reduced liquid-phase salt leaksthrough the development of advanced packing configurations and a self-contained thermal management (STM) system [4], concerns still persist about damage unabated salt vapors can have within salt valves at higher temperatures.

Molten salt freeze events can impact containment reliability when liquid-phase salt expands within a confined area particularly when relatively large thermal gradients are present. This expansion can be particularly problematic around the packing seal or with bellows seals. Kolb et al. [5] found that thawing nitrate salt could result in volume expansion of approximately 5%. Conversely, thermodynamic studies by Campbell Van Der Kouwe [6] demonstrated volumetric expansion of thawing chloride molten salts to be as high as 11.7%. For generation 3 CSP systems [7] this presents a particular challenge considering the operational temperature goals are as high as 720 °C on the hot leg, and freeze recovery events could cause seal and wetted boundary rupture depending on the strength capacity of the containment materials.

An additional issue from the higher operating temperatures of the salts is vapor plating and transmission to cooler parts of the system especially those covered or protected by ullage gas. As valves increase in size the vapor plating issues could be exacerbated by the exposure of larger surface areas to the salt vapor deposits thus affecting the thermal gradients and operation of the valves and supporting monitoring equipment. Here, improved thermal management will be important for ensuring operational reliability. In their study, Kolb et al. [5] also found relatively large thermal gradients experienced across a freeze-thaw piping cross-section revealed variability in the tensile forces and subsequent deflection. For molten salt valves, large thermal gradients across extended bonnet sections of a valve could be subject to large thermal gradients and deflections if proper thermal management is not undertaken. Further, the researchers found within 10 °C across the melting temperature of a HITEC nitrate salt that the expansion facilitated stress levels that exceeded the stainless-steel tensile stress limit to cause cracking.

In this investigation the CFD model investigates a particular FCV designed with both a bellows and packing seal as shown in Fig. 1. The heat transfer fluid (HTF) investigated here considers a 20%NaCl/40%$MgCl_2$/40%KCl by mol. wt. % salt chemistry, which has been shown to have thermal transport challenges at high-temperature (>600 °C) with respect to thermal-mechanical stress corrosion [8], fatigue [9] and MgO precipitation and erosion [10]. Operational challenges with this particular salt chemistry also include vapor formation, where constituent products have been shown by the Gen 3 Liquid-Pathway team [11] to consist of $KMgCl_3$ (carnallite), NaCl, KCl and $MgCl_2$ within a purified salt environment, Table 1. These gaseous molecules after solidification generally have melting

temperatures that are greater than 700 °C, with the exception of the carnallite component which can be as low as 484 °C [12]. This relatively low melting temperature presents a unique challenge considering the melting temperature of the ternary chloride salt is even lower, at a value of approximately 400 °C [11].

Table 1. Product salt vapor component properties.

Gaseous Molecule	Molecular Mass [g/mol]	Melting Temperature [°C]	Diffusivity [m^2/s]	Reference
$KMgCl_3$	169.76	480	2.38E-05	[12]
NaCl	58.44	797	7.45E-05	[11]
KCl	74.55	768	4.62E-05	[11]
$MgCl_2$	95.211	714	6.85E-05	[13]

Unpurified salt, particularly in the presence of water vapor have been previously shown to form Cl^- and HCl which may also have an impact on material integrity and degradation of valve seals. This investigation however will only consider an ideal purified salt without the presence of water vapor reactions and subsequent product formation, as well as dross. For model development ANSYS Fluent (CFD) and Mechanical (FEA) software is employed for characterizing thermal-fluid transport within an FCV valve. First, a CFD model is developed considering liquid-phase fluid transport through the body of the valve with vapor production that is facilitated particularly as the valve is operated between 500 °C and 730 °C.

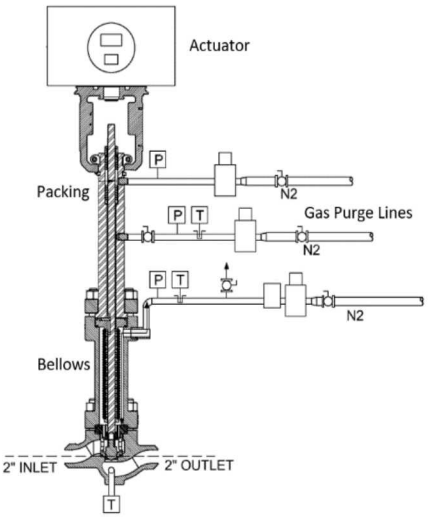

Figure 1. 2 in. flow control valve design with three nitrogen ullage gas lines.

Within the present Gen 3 Liquid-Pathway process flow system design, multiple FCVs are employed where the hot-side unit, which is placed near the base of the downcommer section may experience pressures as high as 150 psig. For the FCV, thermal-fluid transport will take place under this applied pressure where the impacts of vapor pressure rise, and vapor product formation will be considered. This work will subsequently explore molten salt vapor transport through a bellows and packing seals. Within the present FCV configuration, a nitrogen (N_2) purge gas is applied above the seal area to reduce the transport of salt vapors into this region. However, there is much concern that the N_2 purge gas may not restrict salt vapor flow where constituent products, such as $KMgCl_3$ may penetrate further up the valve stem regions and solidify. The melting temperature of this plated material has been shown to be as high as 484.8 °C [14], which is greater than the eutectic melting temperature of the ternary chloride salt mixture at approximately 425 °C [15]. Plated salt vapors have previously been shown to cause reliability issues of subcomponents [16] which may reduce overall service life of the molten salt valve. Therefore, this modeling work will examine phase change phenomena of vapor products and assess stress-related impacts due to plating within possible internal vapor transport sections of the valve.

3. Model Development & Analysis

To accurately capture the complex physics interactions and use of advance model solvers and techniques, especially with respect to large computational costs, a 2D model was developed to consider a two-part phase change model. For

this investigation, the modelling effort considered a contingency operational mode where nitrogen gas pressure and was lost to the ullage gas valve purge lines to characterize plating that would immediately occur. This model was developed to first assess phase change for the salt vapor to a liquid state. The second part of the model considered the liquid phase change to a solid as the nitrogen gas line and salt vapor flow surfaces cooled. Within the volume of fluid (VOF) framework used for this analysis, a pressure-based solver was used along with an Eularian multiphase approach to solve a set of n momentum and continuity equations for each respective phase within each descretised unit cell. Physical coupling within the model is achieved through calculated pressure and interphase exchange coefficnets [17]. Overall, four submodules were inlcuded within the ANSYS Fluent modelling framework. The energy submodel was developed according to Eqn. 1, which considered a transient time step $\partial/\partial t$.

$$\frac{\partial}{\partial t}(\rho E) + \nabla \cdot \left(\vec{v}(\rho E + p)\right) = \nabla \cdot \left(k_{eff} \nabla T\right) \tag{1}$$

where k_{eff} is the effective thermal conductivity, ρ is density, t is time and $\vec{v}$ is the velocity vector. The VOF model framework treats energy, E and the temperature, T as mass-averaged vairables [17]. For an i-phase system, the volume-fraction α is averaged against the respective density based on the form of Eqn. 2 where E_i for each phase is based on the speciic heat of that phase and the shared temperature.

$$E = \frac{\sum_{i=1}^{n} \alpha_i \rho_i E_i}{\sum_{i=1}^{n} \alpha_i \rho_i} \tag{2}$$

For the second laminar fluid dynamics model, a single momentum equiation is solved throughout the modelling domain, resulting in a veolicty feild which is shared amoung both phases i and j. The Eqn. 3 momentum equation is dependent on the volume fractions with reqspect to phase properteies ρ, and viscosity μ.

$$\frac{\partial}{\partial t}(\rho \vec{v}) + \nabla \cdot (\rho \vec{v} \vec{v}) = -\nabla p + \nabla \cdot [\mu(\nabla \vec{v}) + \nabla \vec{v}^T] + \rho \vec{g} \tag{3}$$

Finally, to perform the prediction of phase change from liquid to solid, the ANSYS soldification model was employed where the energy equation takes on a form with respect to enthalpy, H and latent heat, Eqn. 4.

$$\frac{\partial}{\partial t}(\rho H) + \nabla \cdot (\rho \vec{v} H) = \nabla \cdot (k \nabla T) \tag{4}$$

Where the enthalpy of a particular material is calculated by Eqn. 5 and the sum of the sensible enthalpy, h and the latent heat ΔH.

$$H = h + \Delta H \tag{5}$$

In this simulation the focus was set on the two lower nitrgen gas ullage lines and the salt vapor transport flow path above the bellow seal as shwon in Fig. 2a.

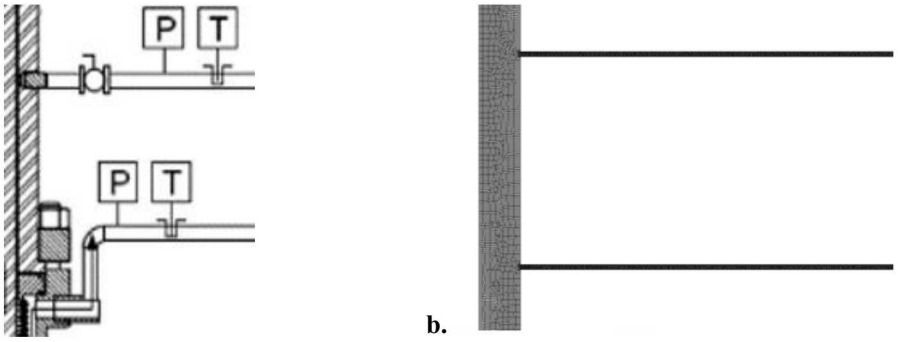

Figure 2. a. Valve control volume considering the two N2 ullage gas lines and the salt vapor transport section, and b. ANSYS Fluent single mesh domain.

This 2D transient CFD simulation was developed to capture phase-change effects throughout all of the possible liquid and gas fluid regions. A converged fine resolution mesh with a characteristic element size of approximately 1 mm and 2 mm was applied to the N_2 gas lines and core valve control volume. Additionally, the transient simulation was fixed with a 0.3 sec. time step to facilitate a Courant number less than one, to ensure flow dynamics convergence. To capture

boundary layer flow dynamics more accurately, the model domain mesh, Fig. 2b included inflation mesh layers were added along the inner wall surfaces. Additionally, no-slip flow boundary conditions were also included. An inlet saturated salt vapor flow condition of approximately 0.01 m/s was applied to approximate laminar flow within the valve. Adiabatic conditions were also applied to the vertical salt vapor transport section. The inlet pipes will also use low mesh resoluation values with inflation layers added along the inside of the pipes to capture boundary layers created by the 5 scfm flowing N_2 gas.

This simulation will allow us to examine the standard operating conditions of the system. The temperature range of the molten salt used in this simulation are between 500 ˚C and 720 ˚C. Although kept constant for this investigation, the inlet pressure of the nitrogen gas and the inlet of the molten salt may also be varied according to minimum and maximum allowable operating conditions.

4. Results

The model results for fully developed flow suggested a constant steady velocity flow profile, shown in Fig. 3 that considered salt vapor flow up the main valve bonnet column, with tributary flow to the N2 ullage gas lines. Since a no-slip boundary condition was employed the fluid was shown to have a zero velocity at the wall surface with a slight increase into the bulk fluid region.

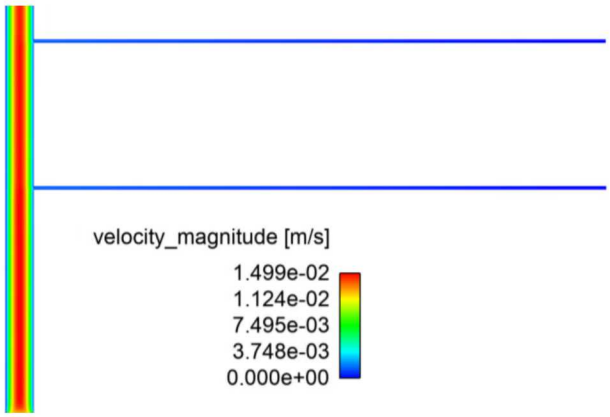

Figure 3. Modelled fluid flow within the valve verictal column and N_2 tributary gas lines.

To characterize the plating phenomena, plating analysis largely focused on assessment of the volume fraction (that has a range between 0 and 1 with respect to phase) for both phase change models. As shown in Fig. 4 for the middle N_2 gas line, the transition from vapor (red) to liquid (blue) was found to completely start closing off the line at approximately 10 sec. Additionally, the phase change was observed to reduce the gas line interface approximately 1 in. from the piping interface. This presents a more opportunistic place to perform maintenance for cutting off the pipe and replacing it with a new welding section. Overall, the molten salt vapor would only occupy a small volume fraction because of small partial pressure within the total gas mixture.

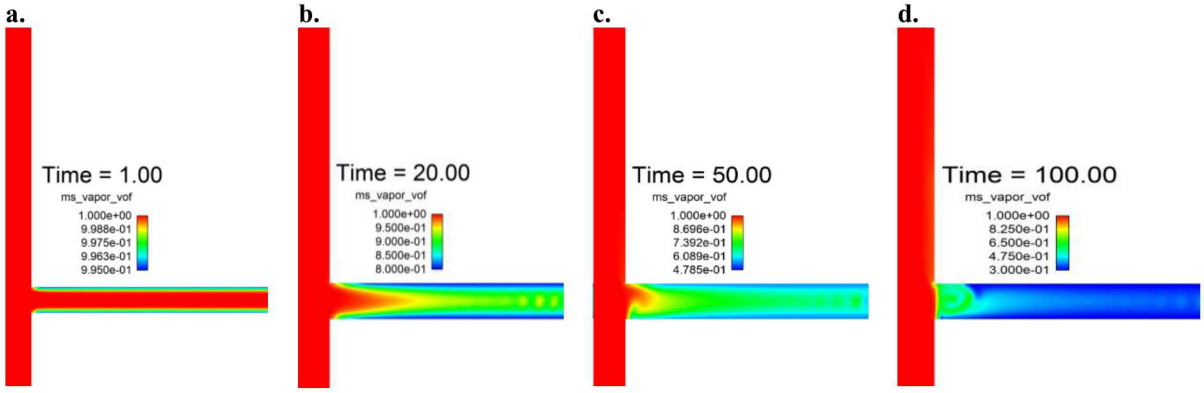

Figure 4. Vapor/liquid VOF phase change model volume fraction results for vapor region (red, = 1) and liquid phase (blue, = 0).

For the second phase change model the analysis was performed in characterizing the solidification of the liquid phase as the temperatures reduced toward the 425 °C melting temperature of the ternary chloride salt. The results, as shown in Fig. 5, for liquid (red) and solid (blue) regions, that the liquid from the previous model would tend to keep its relative position and eventually solidify in the same approximate location as the temperature was allowed to continually decrease.

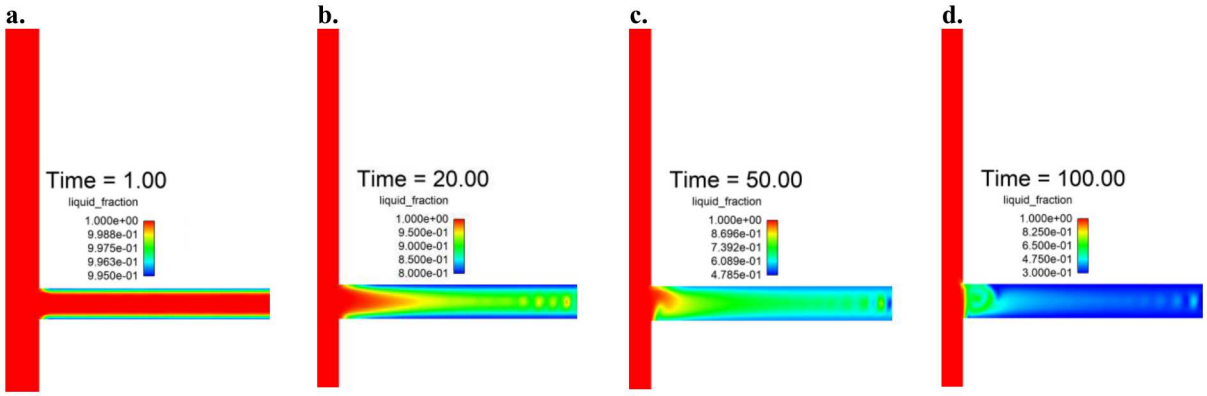

Figure 5. Liquid/Solid Solidification phase change model volume fraction results for liquid region (in red, = 1) and solid region (blue, = 0).

In a larger high-level analysis examining the phase-change plating impacts to both N_2 gas lines, the results suggested a slightly higher velocity found on the bottom gas line which reduce the vapor speed to the top line by as much as ~5%. As shown in Fig. 6 this higher velocity resulted in a further solidification front at approximately 5.6 sec. with respect to the core vertical vapor transport section. However, as the solidification was allowed to continue the front progressively moved to approximately the same location as the top gas line. Overall, the results suggest that a loss in N_2 ullage gas pressure and line heating would result in a near-immediate plating scenario, where total plating would occur within 60 seconds.

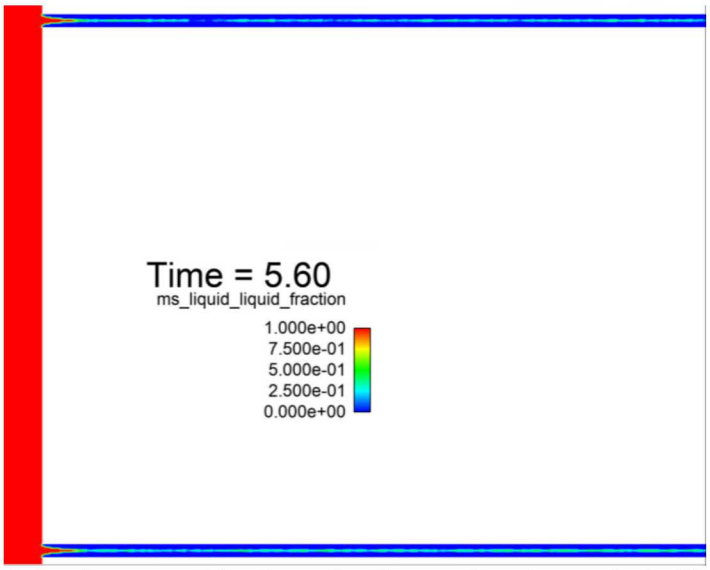

Figure 6. Liquid/Solid phase change model volume fraction results where red signifies the vapor region to a completely blue solid phase.

5. Conclusion

A rigorous analysis was performed for a 2 in. FCV with a ternary chloride molten salt to explore the impacts of phase-change throughout the various stages of the valve, and to assess thermal-mechanical behavior during transiet operation as high as 750 °C. N_2 gas purge lines, can have notable consequences on freeze-conditions for the valve since the purge lines are required to abate salt vapors from transporting up the valve stem to the higher-level packing structures.

The ANSYS Fluent VOF model was developed with consideration of multiple N_2 purge gas lines where the temperature and flow of the incoming fluid will impact salt vapor phase change and subsequent material plating phenomena. This analysis considered successive vapor/liquid and liquid/solid phase change where total plating was observed to occur at approximately 60 seconds. Additinally, increased velocities were found to abate the plating front slightly, however as soldification was allowed to continue, the front locations between both middle and bottom N_2 gas lines were found to effectively be in the same locations. Further research is on-going to parametrically characterize the plating phenomena within a higher fidelity FCV for varying N_2 gas flow rates and pressures, as well as ullage gas line heating profiles. Additionally, this investigation considered the employment of classical thermodynamics modelling to evaluate macroscopic gas dynamics and phase change. Statistical thermodynamics would be required however to capture interactions between product salt vapor constituents and N2 gas speieces to obtain pmore accurate psychometric properties and gas phase change dynamics.

6. Acknowledgements

Sandia National Laboratories is a multimission laboratory managed and operated by National Technology and Engineering Solutions of Sandia, LLC., a wholly owned subsidiary of Honeywell International, Inc., for the U.S. Department of Energy's National Nuclear Security Administration under contract DE-NA0003525.

7. References

1. Smith, D.C., Rush, E.E., Matthews, C.W., Chavez, J.M. and Bator, P.A., 1992. Report on the test of the molten-salt pump and valve loops (No. SAND91-1747). Sandia National Labs., Albuquerque, NM (United States).
2. Gill, D., Kolb, W. and Briggs, R., 2014. An Evaluation of Pressure Measurement Technology and Operating Performance Using Sandia's Molten Salt Test Loop. Energy Procedia, 49, pp.800-809.
3. Pridgen, R.L., Aluminium Company of America, 1984. Method of sampling a liquid in a container. U.S. Patent 4,454,774.
4. Armijo, K.M. 2019, "High-Temperature, Freeze and Leak Resistant Advanced Molten Salt Valve," DOE Proposal DE-FOA-0002064.
5. Kolb, G., Ho, C., Iverson, B., Moss, T. and Siegel, N., 2010, January. Freeze-Thaw Tests on Trough Receivers Employing a Molten Salt Working Fluid. In Energy Sustainability (Vol. 43956, pp. 693-698).
6. Campbell, A.N. and Kouwe, E.V.D., 1968. Studies on the thermodynamics and conductances of molten salts and their mixtures. Part V. The density, change of volume on fusion, viscosity, and surface tension of sodium chlorate and of its mixtures with sodium nitrate. Canadian Journal of Chemistry, 46(8), pp.1279-1286.
7. Ding, W., Shi, H., Jianu, A., Xiu, Y., Bonk, A., Weisenburger, A. and Bauer, T., 2019. Molten chloride salts for next generation concentrated solar power plants: Mitigation strategies against corrosion of structural materials. Solar Energy Materials and Solar Cells, 193, pp.298-313.
8. Cho, S.H., Hur, J.M., Seo, C.S. and Park, S.W., 2008. High temperature corrosion of superalloys in a molten salt under an oxidizing atmosphere. Journal of Alloys and Compounds, 452(1), pp.11-15.
9. Kruizenga, A.M., Andraka, C.E. and Kolb, W.J., 2016. Molten Salt Technology (No. SAND2016-8201PE). Sandia National Lab.(SNL-CA), Livermore, CA (United States); Sandia National Lab.(SNL-NM), Albuquerque, NM (United States).
10. Zhou, H. and Yuan, J.J., 2004. Progress in preparation of high-purity anhydrous magnesium chloride. CHINESE JOURNAL OF PROCESS ENGINEERING., 4(3), pp.281-287.
11. Zhao, Y. and Vidal, J., 2020. Potential scalability of a cost-effective purification method for MgCl2-Containing salts for next-generation concentrating solar power technologies. Solar Energy Materials and Solar Cells, 215, p.110663.
12. JANÁK, G., 2009. INTERACTIONS OF MELT KCl-MgCl2 WITH LINING Al2O3-SiO2-SiC IN METALLURGY OF ALUMINIUM. In *Proceedings of EMC* (p. 1).
13. Singh, D., Kim, T., Zhao, W., Yu, W. and France, D.M., 2016. Development of graphite foam infiltrated with MgCl2 for a latent heat based thermal energy storage (LHTES) system. Renewable Energy, 94, pp.660-667.
14. JANÁK, G., 2009. INTERACTIONS OF MELT KCl-MgCl2 WITH LINING Al2O3-SiO2-SiC IN METALLURGY OF ALUMINIUM. In Proceedings of EMC (p. 1).
15. Mohan, G., Venkataraman, M., Gomez-Vidal, J. and Coventry, J., 2018. Assessment of a novel ternary eutectic chloride salt for next generation high-temperature sensible heat storage. Energy conversion and management, 167, pp.156-164.
16. Sabharwall, P., Ebner, M., Sohal, M. and Sharpe, P., 2010. Molten Salts for High Temperature Reactors: University of Wisconsin Molten Salt Corrosion and Flow Loop Experiments--Issues Identified and Path Forward (No. INL/EXT-10-18090). Idaho National Laboratory (INL).
17. ANSYS Inc., 2011. Fluent 14.0 user's guide. *ANSYS FLUENT Inc.*